AAEC/E604

AAEC/E604

AUSTRALIAN ATOMIC ENERGY COMMISSION

RESEARCH ESTABLISHMENT

LUCAS HEIGHTS RESEARCH LABORATORIES

A NEUTRONICS STUDY OF REDUCED ENRICHMENT FUEL FOR THE HIFAR RESEARCH REACTOR

by

B.V. HARRINGTON

G.S. ROBINSON

JUNE 1985

ISBN 0 642 59806 1

AUSTRALIAN ATOMIC ENERGY COMMISSION
RESEARCH ESTABLISHMENT

LUCAS HEIGHTS RESEARCH ESTABLISHMENT

A NEUTRONICS STUDY OF REDUCED ENRICHMENT FUEL FOR THE HIFAR RESEARCH REACTOR

by

B.V. HARRINGTON
G.S. ROBINSON

ABSTRACT

The neutronics consequences of using lower enrichment fuels for the research reactor HIFAR have been assessed. Comparative results include neutron flux, reactivity performance, plutonium production, and a selection of reactivity coefficients and safety-related parameters for both high and low burn-up of the fuels considered.

National Library of Australia card number and ISBN 0 642 59806 1

The following descriptors have been selected from the INIS Thesaurus to describe the subject content of this report for information retrieval purposes. For further details please refer to IAEA-INIS-12 (INIS: Manual for Indexing) and IAEA-INIS-13 (INIS: Thesaurus) published in Vienna by the International Atomic Energy Agency.

HIFAR REACTOR; FUEL ELEMENTS; REACTOR CORES; ALLOY NUCLEAR FUELS; MODERATELY ENRICHED URANIUM; URANIUM 235; PLUTONIUM; BURNUP; GROUP CONSTANTS; NEUTRON FLUX; REACTIVITY; REACTIVITY COEFFICIENTS; PERFORMANCE; COMPUTERIZED SIMULATION; H CODES

CONTENTS

1. INTRODUCTION

The AAEC's materials testing reactor HIFAR, a D_2O moderated reactor of the DIDO class, uses uranium-aluminium alloy fuel elements with uranium enriched to 80 wt % ^{235}U (HEU). Since supply of this traditional fuel could cease, neutronics calculations have been undertaken to assess the performance and penalties likely to be incurred by the use in HIFAR of fuel enriched to 45 per cent in ^{235}U (MEU), and 20 per cent in ^{235}U (LEU). Economic penalties are not considered.

In this study, the performances of four different reduced enrichment fuel elements are compared with that of the standard HEU HIFAR fuel element. The geometry of this element has been assumed for the reduced enrichment fuel, except that for one element a thicker fuel 'meat' was necessary to achieve the required ^{235}U loading. For most calculations, a uniform burn-up model of HIFAR has been used. Calculations simulating actual HIFAR operation over 21 fuel cycles have been done to confirm the reliability of the results of the uniform burn-up calculations.

2. DESCRIPTION OF THE HIFAR CORE AND FUEL ELEMENTS

HIFAR operates at 10 MW on a 28 day cycle (about 24 days at power) using 25 fuel elements. The fuel elements are on a 152.4 mm square pitch in a 4,6,5,6,4 array with the central row displaced by one half-pitch. The heavy water for the moderator and reflector is contained in a cylindrical aluminium tank, 2 m diameter $\times$ 12.7 mm thick. The bottom of the tank (16 mm thick) is dished but, in RZ models of the reactor, is assumed to be flat providing a bottom heavy water reflector having a uniform thickness of 0.45 m. The top D_2O reflector extends 0.78 m above the active core. Additional radial and bottom reflectors of 0.6 m thick graphite are located outside the tank.

A large number of horizontal beam tubes and vertical facilities extend into the heavy water reflector. All except the small 2 TAN facility have been represented in the calculations. The six 'signal arm' absorbers which control the reactor have, however, not been included.

The standard fuel element consists of four concentric fuel tubes, each of 0.66 mm thick U-Al alloy meat clad in 0.45 mm thick aluminium. The active length is 603 mm. Each fuel tube is made up of three curved plates welded together; the consequent aluminium seams between plates reduce the notional volume available for fuel meat by 9.1 per cent. The inner radii of the fuel tubes are 30.39, 35.29, 40.19 and 45.09 mm. Inner and outer aluminium tubes of inside radii 25.36 and 49.90 mm and thicknesses 1.63 and 1.59 mm, respectively, complete the element and provide five coolant channels of width (inner to outer) 3.4, 3.38, 3.38, 3.38 and 3.29 mm. The standard element contains 150 g ^{235}U at an enrichment of 80 per cent ^{235}U.

Five fuel element types were considered in this study (Table 1). The ^{235}U loading in each of the fuel types with low enrichment was chosen to approximate the reactivity performance of standard fuel. The above fuel element geometry (including the three-plate construction method) was maintained in all cases, except for type 20A fuel where a thicker fuel meat was required (see below). In this case, the mean fuel tube radii were maintained and the coolant channel widths reduced to 3.23, 3.04, 3.04, 3.04 and 3.12 mm (inner to outer).

- Fuel type 80A is the standard HEU fuel with 17 wt % uranium in the meat.
- Fuel type 45A is a 45 per cent ^{235}U enriched element using UAl_x-Al of 29.9 wt % uranium.
- Fuel type 20A, also UAl_x-Al, represents the use of 20 per cent ^{235}U enrichment at the density limit for currently qualified fuel technology, which was taken to be 42 wt % uranium for either UAl_x or U_3O_8-Al. An increase in fuel meat thickness was required to achieve the necessary ^{235}U loading.
- Fuel types 20B (170 g ^{235}U/element) and 20C (160 g ^{235}U/element) are U_3O_8-Al, the long-term fuel material most likely to be favoured, without restriction on uranium density. The cases correspond to 67.1 and 64.9 wt % U_3O_8 respectively.

3. REACTOR MODELS

The standard HIFAR models [Harrington 1983] have been used for both the generation of cross sections and the global calculations. The calculation was performed with modules of the AUS neutronics system [Robinson 1975a]. A brief description of the modules and their application is included below.

3.1 Generation of Cross Sections for Core and Reflector

Cross sections for the core as a function of burn-up were generated using the four AUS modules MIRANDA, ANAUSN, EDIT and CHAR, which are described briefly in turn. A radial model with a circular reflective (white) outer boundary was used to represent the square fuel cell.

MIRANDA [Robinson 1977] is a data preparation code which generates multigroup cross sections for each of the materials in a lattice cell. The code was used with a 128-group cross section library derived from ENDF/B-IV which includes resonance data in the form of subgroup parameters. The resonance calculation is a subgroup method which uses collision probability routines to represent spatial effects. For these problems, nine regions were used in the resonance calculation, with the four fuel-meat tubes represented explicitly. This is considerably more complex than the more usual 3-region (fuel, can, coolant) resonance calculation used in MIRANDA. Some energy condensation was also performed in MIRANDA, which includes a homogeneous spectrum calculation, to produce a 25-group cross section set, of which 15 groups were below 1 eV.

The ANAUSN module [Clancy 1982] is a general purpose, one-dimensional discrete ordinate program. It was used here in an isotropic scattering, S4, 29 mesh interval calculation (maximum interval of 6 mm) using the 25-group data from MIRANDA. All materials were represented explicitly.

The EDIT module [J.P. Pollard, AAEC unpublished report] was used to edit the flux output of ANAUSN to form cell-average cross sections, to perform a homogeneous flux calculation which included a buckling search to give $k_{eff} = 1.08$.

The CHAR module [Robinson 1975b] is a multiregion burn-up module which uses analytic techniques to perform nuclide burn-up using spatial fluxes from other AUS modules. In these calculations, the ANAUSN fluxes adjusted to the EDIT near-critical spectrum were used to form the nuclide depletion equations for each of the four fuel-meat tubes. Burn-up was performed at a constant thermal flux which was set to give an average power of 10/25 MW per element. All results are given with a xenon level corresponding to this flux level.

Repeated cycles through the above four modules were made to generate actinide and fission product concentrations. Linear interpolation in ^{235}U mass was used to get concentrations at the required burn-up values. Fuel cell calculations using these concentrations and the modules MIRANDA, ANAUSN and EDIT generated 5-group cell-average cross sections. This indirect method was adopted so that cross sections could be obtained for a set of perturbations in cell temperatures and densities. Five-group cross sections for the heavy water and graphite reflectors were generated separately in MIRANDA by condensation over the flux obtained from a ^{235}U fission source in each material. The energy boundaries were 0.82 MeV, 9.12 keV, 1.13 eV and 0.14 eV.

3.2 Global Calculations

The XY flux calculations were performed in the POW module [Pollard 1974] which is a two-dimensional, finite difference code using edge mesh points.

The XY HIFAR model [Harrington 1983] includes a detailed representation of both horizontal and vertical facilities in the heavy water reflector and a typical rig loading. It was necessary to include this detail to achieve criticality in the calculations and obtain reasonable flux distributions. Although such detail is not essential here, it is preferable for reactors with large amounts of reactivity invested in rig loading and fuel burn-up, that the rig burden be included directly in the calculation.

The horizontal beam tubes were the most difficult facilities to represent, and were treated by an approximate model, with the results normalised to an RZ S_n DOT [Rhoades and Mynatt 1973] calculation of the major 10H beam tube. The reactivity worth of the radial reflector facilities included in this way is 5 per cent. An additional reactivity worth of 2.2 per cent (measured value) for reflector

rigs was included by inserting the required amount of thermal absorber at the rig locations. A typical in-core rig loading of 2.3 per cent spread over five fuel elements was also simulated by insertion of localised thermal absorbers.

Bucklings for the XY geometry calculations were obtained from RZ calculations which included smeared representations of the structure in the radial and axial heavy water reflectors. Centre-plane bucklings were used throughout in preference to core-height-average bucklings. This implies that the fluxes quoted are for the mid-height plane, and they have been so normalised.

The reactivity scale used requires some explanation. Instead of the normal definition of percentage reactivity, *i.e.* $\rho = 100\ (1 - 1/k_{eff})$, it is practice with HIFAR operational data to use a percentage reactivity, ρ' which is the equivalent reactivity in a core containing 3.2 kg of ^{235}U. This has the advantage that the change in ρ' due to a rig, making a fuel change or moving the control arms is independent of the fuel loading. The relationship used to derive calculated ρ' values is

$$\rho' = \rho\ (M/3.2)^{0.7}$$

where M is the reactor ^{235}U loading in kg. When comparing fuels of various enrichment, however, it is necessary to allow for the ^{239}Pu as well as the ^{235}U loading. To account for the higher cross section of ^{239}Pu, twice the ^{239}Pu mass has been added to the ^{235}U mass to obtain an 'equivalent ^{235}U' mass. The reactivities given in the preceding paragraphs are ρ' values derived in this way.

The reactor models outlined above have been checked by comparison with the end-of-cycle core state for a particular HIFAR operating program (OP 251). For this comparison, the core state calculated using the simple fuel accounting program HIBURN [McCulloch and Trimble 1969] was used. The excess ρ' held in the control arms was calculated to be 1.49 per cent using the explicit burn-up of individual fuel elements, and 0.84 per cent using a uniform core burn-up, compared with 1.43 per cent actually observed.

The basic results reported here are for cores of uniform burn-up. This approach was used for simplicity, and its accuracy is considered in Section 5.

4. BASIC RESULTS

HIFAR fuel cycle data averaged over the last 21 operating programs are presented in Table 2. It is evident that at present the rig burden is low, and the fuel burn-up correspondingly high. The fuel management scheme involves loading most new elements near the core centre and moving elements outward (after a delay of at least one cycle out of reactor for cooling).

Because the rig burden of HIFAR may vary considerably in the future, we have chosen to consider two cases which cover the likely range. The first is based on the core state at the end of OP 251, which had an average burn-up of 45.16 MWd/element and an in-core rig ρ' of 2.3 per cent. The second has a burn-up of 33.68 MWd/element and an in-core rig ρ' of 6.2 per cent (the extra 3.9 per cent being added to give the same k_{eff} for standard HEU fuel). The extra rig burden was represented by a uniform thermal absorber in the 20 elements not already having an explicit rig loading.

The results obtained from XY calculations using bucklings from the appropriate RZ calculations are given in Table 3. The ρ' values derived from these cases are summarised in Table 4. The columns labelled 'high' and 'low' burn-up give the excess ρ' values for the two situations. They show that:

(a) all the chosen reduced enrichment cases have a similar or higher reactivity than standard fuel over this burn-up range; and

(b) the reactivity performance of low enrichment fuel is better at high burn-up than at low burn-up.

Additional calculations for the low burn-up cases were made without the extra rigs, and the results used to give the rate of change of ρ' with burn-up (Table 4). These values can be interpreted as the rate of reactivity loss (excluding transient effects) within a program, and demonstrate that the control required to balance this loss is smaller for the low enrichment fuels.

The axial form factors for the thermal flux and the average core centre-plane thermal fluxes are given in Table 5 for all cases. The thermal flux used throughout is the Westcott flux. The reductions in core thermal flux are about 7, 20 and 13 per cent for 45A, 20A and 20C fuel, respectively. Further information on the flux changes in the high burn-up cases is given in Figures 1 to 4 where fluxes along the X-axis for 80A fuel and flux ratios for the other fuels are given. In these graphs, the fast flux is > 0.8 MeV and the epithermal flux is from 9.1 keV to 1.1 eV.

A selection of reactivity coefficients and other safety related parameters which have been calculated by perturbation theory are compared in Tables 5 and 6. The fuel coefficient for the central element gives the change in $\delta k/k$ per g of ^{235}U burnt and includes all long term burn-up effects. The absorber coefficients vary considerably but this results mainly from the change in fuel loading and there is a much smaller variation in values of ρ' per cm^2. The prompt neutron lifetime, $\bar{\ell}$, also shows some variation with fuel loading. The small changes in the effective delayed neutron fraction β_{eff} are due to the variation in the ^{239}Pu contribution. Only one set of values is given for the remaining coefficients in Table 6 as the variation with burn-up is less than 3 per cent. There is a considerable increase in the fuel temperature coefficient ($\delta k/k$ per °C) with decreasing enrichment but this coefficient is of minor importance. The fuel plus coolant temperature coefficient is the coefficient for constant coolant density and must be combined with a density change and the void coefficient to obtain a total temperature coefficient. The temperature coefficient and void coefficient ($\delta k/k$ per percentage void) both have minor changes with fuel type. The worth of the top reflector was also calculated for 80A and 20C fuel. The values obtained for changes in ρ' were 9.2 and 10.5 per cent for 80A and 20C fuel, respectively, and the worths of the first 0.2 m of top reflector were 6.6 and 7.6 per cent, respectively.

The power distribution within the fuel element for the various fuels is given in Table 7. The results are for zero burn-up and the distributions flatten slightly as burn-up proceeds. The results are practically identical for all cases.

Plutonium production figures are given in Table 8 for a range of burn-up which covers the anticipated discharge values.

5. CALCULATIONS SIMULATING ACTUAL OPERATION

To supplement the information obtained from a comparison of cores of uniform burn-up, some limited calculations directly simulating HIFAR operation have been done. These have not been performed by the direct use of the general purpose reactor physics methods used in the preceding sections, but with a program similar to the HIBURN program used for HIFAR fuel management. This program, HIFUEL, retains the HIBURN approach of using flux factors and reactivity coefficients, but uses calculated values throughout rather than experimentally based data, and includes a treatment of saturating fission products.

The comparison has been made over the 21 operating programs which gave the average fuel cycle data of Table 2. The fuel movements and time at power have been followed with a constant three-day shutdown between programs. The seven programs before this were also followed but have not been included in the averages because they served as a transition period when the fuel loading rate was changed. The standard fuel has been compared only with 20A fuel, which is the most extreme case.

A summary of the results is given in Table 9. Case 1 represents the actual HIFAR situation. Case 2 represents a situation with high rig burden in which the extra 4 per cent in reactivity has been obtained by increasing the fuelling rate by 50 per cent. A 50 per cent increase was chosen as this could be modelled by maintaining the same average cycle length but making in every two cycles the fuel changes that in case 1 were made in three. In case 3, the power was raised to 15 MW and the refuelling rate was twice that of case 1 (again chosen for simplicity); this resulted in 2.1 per cent extra reactivity using standard fuel. Case 3 has been included because HIFAR uprating may be considered as a future option.

The results show that:

(i) The change from standard to 20A fuel causes a change in end-of-cycle ρ' which is, in each case, about 0.2 per cent above that inferred from the corresponding uniform core calculation.

(ii) The use of 20A fuel has little effect on the total change in ρ' over the operating program. This is because a smaller loss due to fuel burn-up is compensated by a larger loss due to saturating fission products.

It is inferred from these results that the uniform burn-up results may be used with confidence for all fuel types, and that operation at 15 MW introduces no untoward additional difference between fuel types.

6. CONCLUSIONS

The performance of HIFAR, 80 per cent enriched, 150 g ^{235}U fuel elements is reasonably well matched in terms of reactivity by:

(a) 45 per cent enriched ^{235}U elements containing 155 g ^{235}U as UAl_x-Al at $\sim$ 1.0 g cm^{-3} U. No change in fuel element geometry is required, and the fuel technology is within the range in use (in different geometries) in some other high performance reactors.

(b) 20 per cent enriched ^{235}U elements containing 170 g ^{235}U as UAl_x-Al at $\sim$ 1.6 g cm^{-3} U. This density is at the upper limit of fully qualified technology, and would require a change in fuel element geometry (thicker plates) which would reduce thermohydraulic safety margins.

(c) 20 per cent enriched ^{235}U elements containing 160 g ^{235}U as U_3O_8-Al at $\sim$ 2.3 g cm^{-3} U. No fuel element geometry change is entailed, but the fuel technology has yet to be fully developed and qualified.

The largest performance penalty in the use of reduced enrichment fuel comes from the reduced core thermal flux, and is substantial at the 20 per cent ^{235}U level. There are no particularly significant changes in safety related neutronics parameters.

7. REFERENCES

Clancy, B.E. [1982] - ANAUSN — a one-dimensional multigroup S_n transport theory module for the AUS reactor neutronics system. AAEC/E539.

Harrington, B.V. [1983] - Neutronic models for the HIFAR reactor. AAEC/E571.

McCulloch, D.B. and Trimble, G.D. [1969] - A method of estimating fuel burn-up and higher isotope production in the reactor HIFAR. AAEC/TM508.

Pollard, J.P. [1974] - AUS module POW — a general purpose 0, 1 and 2D multigroup neutron diffusion code including feedback-free kinetics. AAEC/E269.

Rhoades, W.A. and Mynatt, F.R. [1973] - The DOT III two-dimensional discrete ordinates transport code. ORNL-TM-4280.

Robinson, G.S. [1975a] - AUS — the Australian modular scheme for reactor neutronic computations. AAEC/E369.

Robinson, G.S. [1975b] - AUS burn-up module CHAR and the associated STATUS data pool. AAEC/E372.

Robinson, G.S. [1977] - AUS module MIRANDA — a data preparation code based on multiregion resonance theory. AAEC/E410.

TABLE 1
FUEL DESCRIPTION

Fuel Type	Fuel Meat	Enrichment (wt %)	^{235}U/Element (g)	Uranium Density (g cm^{-3})	Fuel Meat Thickness (mm)
80A	U-Al alloy	80	150	0.535	0.66
45A	UAl_x-Al	45	155	0.984	0.66
20A	UAl_x-Al	20	170	1.60	1.00
20B	U_3O_8-Al	20	170	2.43	0.66
20C	U_3O_8-Al	20	160	2.28	0.66

TABLE 2
AVERAGE FUEL CYCLE DATA

In-core rigs, ρ'	2.79%
Reflector rigs, ρ'	2.19%
Excess ρ' at shutdown	1.64%
Power	10 MW
Energy per program	227.8 MWd
New fuel elements per program	3.52
Discharge burnup per element	64.7 MWd
Average burnup per element at shut down	40.5 MWd
^{235}U loading at shutdown	2.48 kg

TABLE 3
CASE DESCRIPTION AND k_{eff}

Fuel Type	Fissile Mass (kg)	Burnup MWd/Element	In-core Rig Burden (ρ'%)	k_{eff}	Reactivity (ρ%)
80A	2.3611	45.16	2.32	1.01054	1.04
80A	2.7144	33.68	6.22	1.01047	1.04
45A	2.5953	45.16	2.32	1.01626	1.60
45A	2.8937	33.68	6.22	1.01275	1.26
20A	3.0470	45.16	2.32	1.01820	1.79
20A	3.3583	33.68	6.22	1.01047	1.04
20B	3.0473	33.68	6.22	1.02708	2.64
20C	2.7939	45.16	2.32	1.01564	1.54
20C	3.1061	33.68	6.22	1.00880	0.87

TABLE 4
REACTIVITIES

Fuel Type	ρ% High Burnup	ρ% Low Burnup	$\Delta(\rho\%)/\Delta$ (MWd/Element)
80A	0.84	0.92	0.347
45A	1.38	1.17	0.322
20A	1.73	1.07	0.287
20B		2.73	
20C	1.40	0.85	0.294

TABLE 5
BURNUP-DEPENDENT PARAMETERS

Case	Centre Element: Fuel Coeff. $\delta k/k$ per g of ^{235}U burnt $\times 10^{-4}$	Centre Element: Absorber Coeff. $\delta k/k$ per cm^2	Thermal Flux: Centre-plane Average	Thermal Flux: Axial Form Factor	(sec)	β_{eff}
High Burnup						
80A	-2.066	-2.946×10^{-4}	1.113×10^{14}	1.044	6.44×10^{-4}	6.92×10^{-3}
45A	-1.831	-2.763×10^{-4}	1.033×10^{14}	1.038	6.24×10^{-4}	6.82×10^{-3}
20A	-1.438	-2.370×10^{-4}	0.880×10^{14}	1.022	5.80×10^{-4}	6.70×10^{-3}
20C	-1.596	-2.554×10^{-4}	0.952×10^{14}	1.031	5.98×10^{-4}	6.68×10^{-3}
Low Burnup						
80A	-1.814	-2.635×10^{-4}	0.976×10^{14}	1.037	5.90×10^{-4}	6.94×10^{-3}
45A	-1.647	-2.500×10^{-4}	0.920×10^{14}	1.032	5.76×10^{-4}	6.86×10^{-3}
20A	-1.330	-2.202×10^{-4}	0.803×10^{14}	1.017	5.44×10^{-4}	6.76×10^{-3}
20C	-1.452	-2.352×10^{-4}	0.862×10^{14}	1.026	5.58×10^{-4}	6.75×10^{-3}

TABLE 6
REACTIVITY COEFFICIENTS
($\delta k/k$ per fuel element)

Fuel Type	Core Average: Fuel Temperature	Core Average: Fuel and Coolant Temperature	Core Average: Coolant Void	Centre Element: Fuel Temperature	Centre Element: Fuel and Coolant Temperature	Centre Element: Coolant Void
80A	-0.4×10^{-7}	-3.6×10^{-6}	-3.5×10^{-5}	-0.6×10^{-7}	-5.4×10^{-6}	-5.4×10^{-5}
45A	-3.1×10^{-7}	-3.7×10^{-6}	-3.4×10^{-5}	-5.4×10^{-7}	-5.4×10^{-6}	-5.2×10^{-5}
20A	-6.9×10^{-7}	-3.4×10^{-6}	-3.0×10^{-5}	-12.5×10^{-7}	-4.9×10^{-6}	-4.6×10^{-5}
20C	-7.2×10^{-7}	-3.8×10^{-6}	-3.2×10^{-5}	-12.8×10^{-7}	-5.6×10^{-6}	-4.9×10^{-5}

TABLE 7
POWER FRACTION BY FUEL RING

Fuel Type	Power Fraction			
	Annulus 1	Annulus 2	Annulus 3	Annulus 4
80A	0.194	0.225	0.266	0.315
45A	0.198	0.227	0.264	0.312
20A	0.197	0.226	0.263	0.313
20C	0.197	0.226	0.264	0.313

TABLE 8
PLUTONIUM PRODUCTION

Fuel Type	Burnup MWd/element	Plutonium Production g/element	Isotopic Composition (wt %)			
			^{239}Pu	^{240}Pu	^{241}Pu	^{242}Pu
80A	45	0.58	82.8	13.2	3.6	0.3
	55	0.66	78.5	15.8	5.2	0.6
	65	0.73	73.9	18.2	6.8	1.1
45A	45	1.93	83.6	12.7	3.4	0.3
	55	2.22	79.5	15.2	4.8	0.5
	65	2.46	75.3	17.5	6.3	1.0
20A	45	4.20	84.9	11.7	3.1	0.2
	55	4.89	81.5	13.8	4.3	0.4
	65	5.51	78.0	15.8	5.5	0.7
20C	45	4.09	84.2	12.2	3.2	0.3
	55	4.75	80.5	14.5	4.5	0.5
	65	5.32	76.8	16.6	5.8	0.8

TABLE 9
DIRECT SIMULATION — AVERAGE RESULTS

	Case 1	Case 2	Case 3
Case Description			
Power (MW)	10	10	15
Refuelling rate (elements/program)	3.52	5.28	7.04
ρ' increase *cf* Case 1 for 80A fuel (%)	-	4.00	2.14
Results			
ρ' loss per cycle for 80A fuel (%)	5.71	6.02	7.50
ρ' loss per cycle for 20A fuel (%)	5.79	6.09	7.41
Increase in end of cycle ρ' for change from 80A to 20A fuel (%)	0.80 (0.59)*	0.07 (-0.18)*	0.30 (0.15)*

* Corresponding end of cycle ρ' derived from Table 4

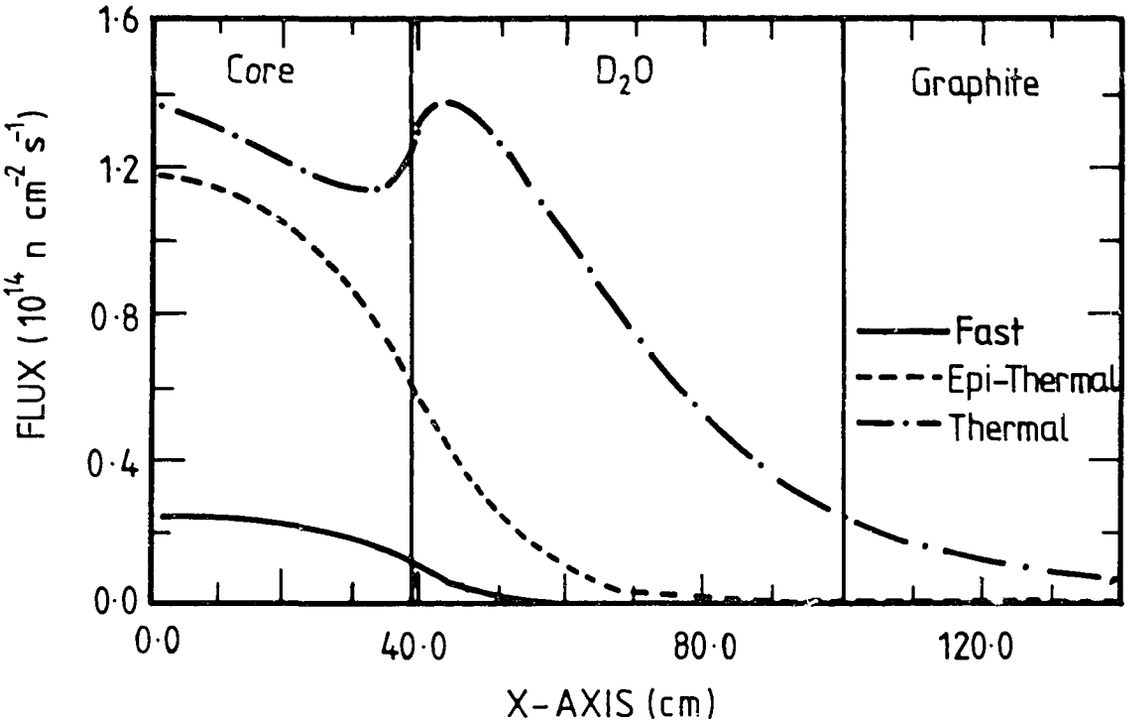

Figure 1 Fluxes at core mid-plane for 80A fuel

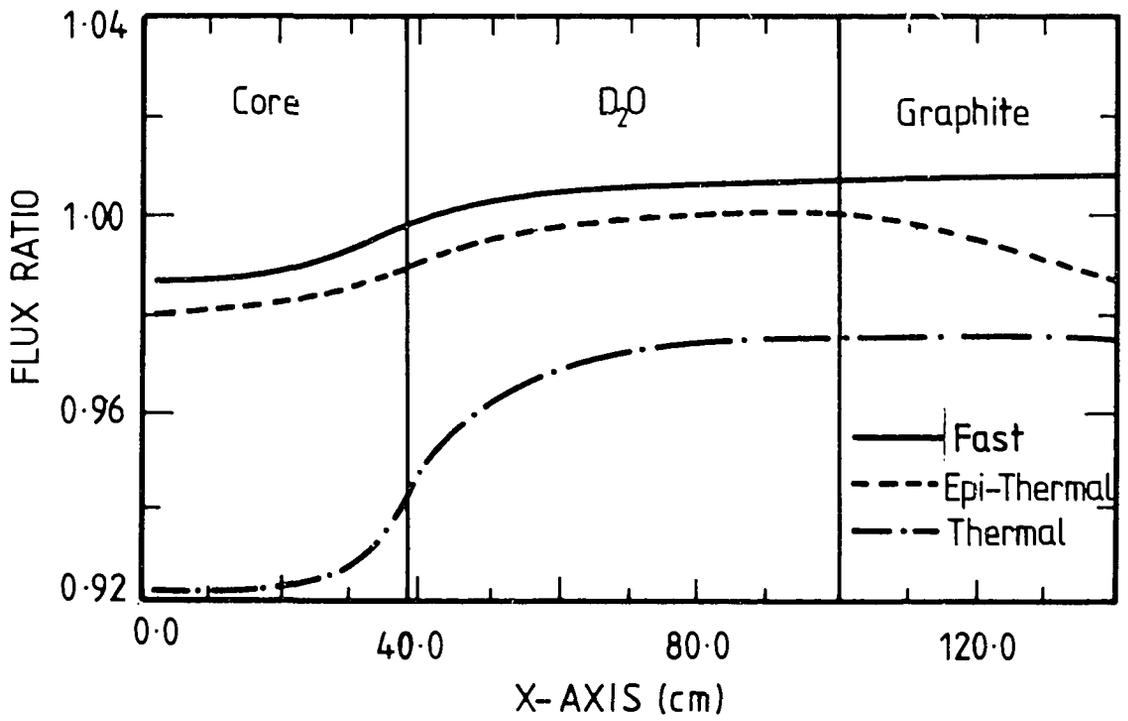

Figure 2 Flux ratios at core mid-plane 45A/80A fuel

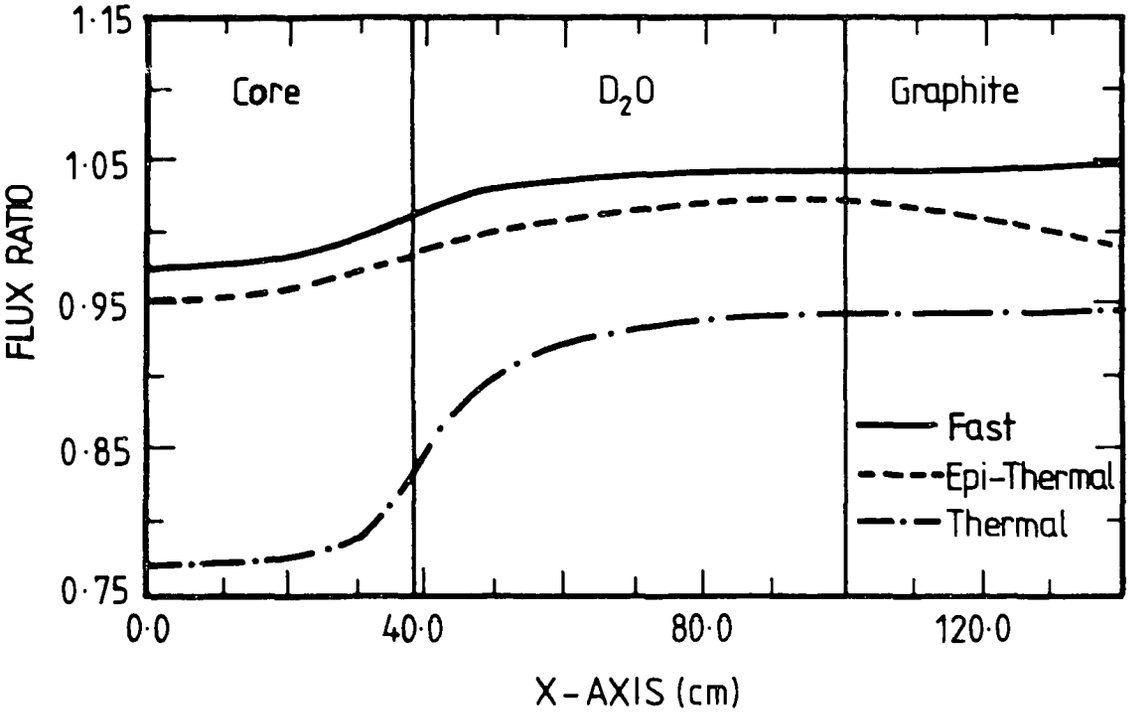

Figure 3 Flux ratios at core mid-plane 20A/80A fuel

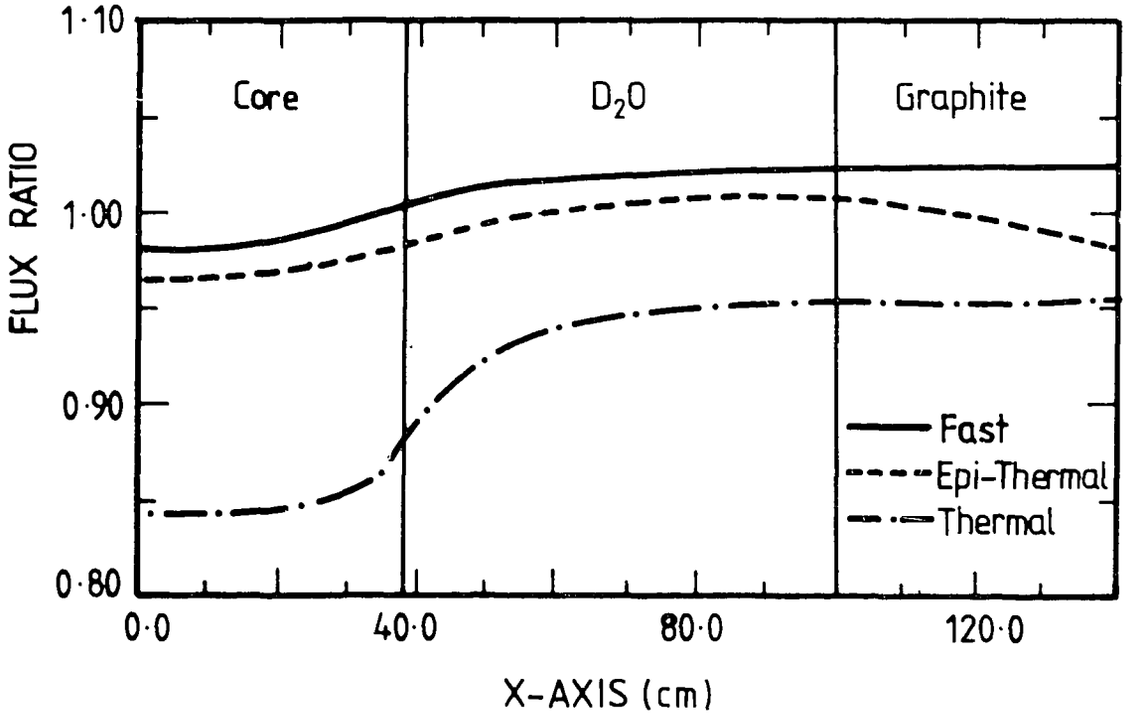

Figure 4 Flux ratios at core mid-plane 20C/80A fuel